Organometallics **1993,** *12,* 1543–1552 1543

Phosphine Adducts of the Open Metallocenes of Zirconium, Hafnium, Niobium, and Molybdenum: Syntheses, Structures, and Reactions with Carbon Monoxide

Thomas E. Waldman, Lothar Stahl, David R. Wilson, Atta M. Arif,
John P. Hutchinson, and Richard D. Ernst*

Department of Chemistry, University of Utah, Salt Lake City, Utah 84112

Received October 23, 1992

The reactions of $MCl_4(PEt_3)_2$ complexes (M = Zr, Hf, Nb, Mo) with 4 equiv of $K(2,4\text{-}C_7H_{11})$ lead to the formation of $M(2,4\text{-}C_7H_{11})_2PEt_3$ complexes. Other related phosphine adducts may be prepared similarly, while phosphite complexes may be prepared by ligand substitution reactions. For the zirconium phosphine complex, exposure to CO generates both the monocarbonyl and the dicarbonyl complexes. Structural data have been obtained for three of the $M(2,4\text{-}C_7H_{11})_2PEt_3$ complexes (M = Zr, Nb, Mo), as well as for $Zr(2,4\text{-}C_7H_{11})_2(CO)_n$ (n = 1, 2). The $M(2,4\text{-}C_7H_{11})_2PEt_3$ complexes for M = Zr and Nb are isomorphous, adopting space group $P\bar{1}$ with $Z = 2$ and respective cell constants of a = 7.988(4) Å, b = 8.631(4) Å, c = 15.649(7) Å, α = 87.98(4)°, β = 103.46(4)°, γ = 91.70(4)°, and V = 1048.3(8) Å^3, and a = 7.936(2) Å, b = 8.735(2) Å, c = 15.511(5) Å, α = 87.82(2)°, β = 103.79(2)°, γ = 92.12(2)°, and V = 1043.0(5) Å^3. Crystals of the molybdenum complex are orthorhombic, belonging to space group $Pbca$ with a = 11.244(2) Å, b = 14.516(2) Å, c = 24.963(4) Å, and V = 4074.5(11) Å^3 for Z = 8. Crystals of the zirconium monocarbonyl complex are also orthorhombic, adopting space group $P2_12_12_1$, with a = 11.827(2) Å, b = 12.158(2) Å, c = 10.328(2) Å, and V = 1485.1 Å^3 for Z = 4. Crystals of the dicarbonyl are triclinic, space group $P\bar{1}$, with a = 8.552(3) Å, b = 9.243(3) Å, c = 20.419(8) Å, α = 93.34(3)°, β = 83.88(3)°, γ = 87.97(3)°, and V = 1600.7 Å^3 for Z = 4 (two independent molecules). Except for the molybdenum complex, all mono(ligand) adducts possess the expected syn-eclipsed oriented dienyl ligands. The molybdenum complex is unusual, having one η^5-S (S = sickle) bound dienyl ligand, while the zirconium dicarbonyl has an unsymmetric orientation of two η^5-U bound ligands, with one carbonyl by the open edge of one dienyl ligand, the other carbonyl being by the backside of the other dienyl ligand.

A number of open metallocenes of the formula $M(2,4\text{-}C_7H_{11})_2$ have been reported for the first-row transition metals titanium, vanadium, chromium, and iron.[1] In contrast, related open metallocenes in the second and third rows seem restricted to ruthenium[2] and osmium,[3] which form 18-electron complexes. Such a situation is quite reminiscent of the metallocene series, for which the 18-electron configuration is required for stability in the second and third row. In order to isolate earlier bis(pentadienyl)-complexes for the second- and third-row transition metals, it appeared that the presence of at least one additional Lewis base would be required, and a preliminary report has appeared in which $M(2,4\text{-}C_7H_{11})_2PEt_3$ complexes of zirconium, niobium, and molybdenum are described.[4] We now present a full report on these species, their hafnium analogs, and additional phosphine and carbonyl complexes.

Experimental Section

General Procedures. The compounds described herein are mostly air-sensitive. They are therefore prepared, handled, and stored under nitrogen or in a glovebox, while solutions are manipulated under nitrogen or CO. Hydrocarbon and ethereal solvents are predried and distilled under nitrogen from Na/benzophenone prior to use. Magnetic and spectroscopic data were obtained as previously described.[5] The starting dienes,[6] dienyl anions,[1] metal complexes, phosphines,[7] and phosphites are either purchased or prepared by standard methods.

$Zr(2,4\text{-}C_7H_{11})_2P(C_2H_5)_3$. A 250-mL, three-neck flask is equipped with a magnetic stirring bar, nitrogen inlet, and pressure-equalizing dropping funnel. The flask is charged with 1.13 g (3.00 mmol) of $ZrCl_4(THF)_2$[8] and 50 mL of THF. A solution of 1.61 g (12.0 mmol) of potassium 2,4-dimethylpentadienide in 50 mL of THF is prepared in the dropping funnel. The flask is cooled to −78 °C, and 0.89 mL (6.0 mmol) of triethylphosphine is added to the zirconium tetrachloride solution by syringe. The potassium salt is added dropwise over a period of 10 min. On warming, the reaction mixture first turns red, then brown, and finally a very deep green-brown. After the solution has reached room temperature, it is allowed to stir for an additional 6 h. The THF is removed under vacuum to give a dry, green and brown solid. Extraction of this residue with several 50-mL portions of pentane results in a green-brown solution which is filtered through a Celite pad on a coarse frit. The solution is reduced to 40 mL in vacuo and then cooled to −20 °C. After 3 days 0.540 g (1.35 mmol) of dark green crystals of bis(2,4-dimethylpentadienyl)-(triethylphosphine)zirconium are isolated (mp 141–142 °C dec). The yield is 45% based on $ZrCl_4(THF)_2$. Yields of 70% could be obtained in reactions using 1 equiv of PEt_3.

^{1}H NMR (benzene-d_6 ambient): δ 4.39 (s, 2 H, H(3)), 2.67 (s, 4 H, H_x(1,5)), 1.74 (s, 12 H, CH_3), 1.44 (m, 6 H, PCH_2CH_3), 1.00

---

[1] Wilson, D. R.; Stahl, L.; Ernst, R. D. *Organomet. Synth.* **1986,** *3,* 136.

[2] Stahl, L.; Ernst, R. D. *Organometallics* **1983,** *2,* 1229.

[3] Stahl, L.; Ma, H.; Ernst, R. D.; Hyla-Kryspin, I.; Gleiter, R.; Ziegler, M. L. *J. Organomet. Chem.* **1987,** *326,* 257.

[4] Stahl, L.; Hutchinson, J. P.; Wilson, D. R.; Ernst, R. D. *J. Am. Chem. Soc.* **1985,** *107,* 5016.

[5] Newbound, T. D.; Stahl, L.; Ziegler, M. L.; Ernst, R. D. *Organometallics* **1990,** *9,* 2962.

[6] Jitkow, O. N.; Bogert, M. T. *J. Am. Chem. Soc.* **1941,** *63,* 1979.

[7] (a) Wolfsberger, W.; Schmidbaur, H. *Synth. React. Inorg. Met.-Org. Chem.* **1974,** *4,* 149. (b) Markham, R. T.; Dietz, E. A.; Martin, D. R. *Inorg. Synth.* **1976,** *16.* (c) Verkade, J. G.; McCarley, R. E.; Hendricker, D. G.; King, R. W. *Inorg. Chem.* **1965,** *4,* 228.

[8] Manzer, L. E. *Inorg. Synth.* **1982,** *21,* 135.

0276-7333/93/2312-1543$04.00/0 © 1993 American Chemical Society

(m, 9 H, PCH_2CH_3), 0.42 (t, 4 H, J = 4.4 Hz, $H_n(1,5)$). ^{13}C NMR (benzene-d_6, ambient): δ 116.3 (s), 97.1 (d, J = 155 Hz), 52.0 (t, J = 150 Hz), 29.1 (q, J = 126 Hz), 17.9 (t, J = 129 Hz), 7.8 (q, J = 127 Hz). $^{31}P\{^1H\}$ NMR (THF, ambient): δ 27.7. Anal. Calcd for $C_{20}H_{37}PZr$: C, 60.10; H, 9.33. Found: C, 60.03; H, 9.36.

$Zr(2,4\text{-}C_7H_{11})_2P(OCH_3)_3$. This compound is easily prepared from the triethylphosphine adduct described above. A 100-mL, two-neck flask equipped with a magnetic stirring bar and nitrogen inlet is charged with 100 mg (0.25 mmol) of bis(2,4-dimethylpentadienyl)(triethylphosphine)zirconium and 50 mL of pentane. A large excess (1.0 mL, 6.5 mmol) of trimethyl phosphite (Aldrich) is added via syringe to the stirred green-brown solution, resulting in an instant color change to bright green. (In case a white solid precipitates the solution must be filtered at this point.) The solution is stirred for an additional 10 min, and the volume is reduced to 30 mL under vacuum. After 3 days at −98 °C, 98 mg (0.24 mmol) of dark green crystals (mp 115–116 °C) of the title compound are isolated. This corresponds to a 96% yield based on $Zr(2,4\text{-}C_7H_{11})_2[P(C_2H_5)_3]$.

^1H NMR (benzene-d_6, ambient): δ 4.53 (s, 2 H, H(3)), 3.49 (d, 9 H, J = 9.4 Hz, $POCH_3$), 2.91 (t, 4 H, J = 2.8 Hz, $H_x(1,5)$), 1.71 (s, 12 H, CH_3), 0.64 (t, 4 H, J = 5.3 Hz, $H_n(1,5)$). $^{13}C\{^1H\}$ NMR (benzene-d_6, ambient): δ 115.6 (s), 97.2 (d), 52.9 (d, J_{P-C} = 5 Hz), 50.5 (t), 28.7 (q). $^{31}P\{^1H\}$ NMR (benzene-d_6, ambient): δ 202.2. Anal. Calcd for $C_{17}H_{31}O_3PZr$: C, 50.10; H, 7.67. Found: C, 49.98; H, 7.66.

$Zr(2,4\text{-}C_7H_{11})_2(P(CH_3)_2(C_6H_5))$. To a 250-mL, three-neck flask equipped with a nitrogen inlet, pressure-equalizing dropping funnel, and magnetic stirring bar are added 3.00 g (7.95 mmol) of $ZrCl_4(THF)_2$ and 100 mL of THF. Dimethylphenylphosphine (1.13 mL, 7.95 mmol) is added via syringe and the resulting heterogeneous mixture cooled to −78 °C. Potassium 2,4-dimethylpentadienide (4.38 g, 32.6 mmol) in 80 mL of THF is added dropwise to the cold suspension over 20 min, during which time the reaction mixture steadily darkens, assuming a blood-red color upon completion of the addition. Following the removal of the cold bath and stirring at room temperature for 2 h, the color changes from red to dark green-brown and the solvent is removed in vacuo. The resulting green-brown solid is extracted with three 100-mL portions of diethyl ether and filtered through a Celite pad on a coarse frit. Concentration in vacuo of the dark green filtrate to approximately 100 mL and cooling to −20 °C overnight yield 2.67 g (6.4 mmol, 62%) of dark green microcrystalline $Zr(2,4\text{-}C_7H_{11})_2PMe_2Ph$. Further concentration and cooling of the mother liquor result in an additional 0.78 g (1.86 mmol) of product for an overall yield of 85% based on $ZrCl_4(THF)_2$. The green-black crystals (mp 158–161 °C dec) are highly air-sensitive, smoldering upon exposure to the atmosphere, and smell strongly of dimethylphenylphosphine.

^1H NMR (benzene-d_6, ambient): δ 7.37–7.01 (m, 5 H, Ph), 4.44 (s, 2 H, H(3)), 2.62 (s, 4 H, H(1,5exo)), 1.67 (s, 12 H, CH_3–PD), 1.47 (d, 6 H, J = 6 Hz, PCH_3), 0.21 (t, 4 H, J = 5.2 Hz, H(1,5endo)). ^{13}C NMR (benzene-d_6, ambient): δ 129.7 (d of d, 1 C, J = 110.4, 9.0 Hz, P*Ph*), 128.8–127.9 (m, 5 C, P*Ph*), 115.9 (s, 4 C, C(2,4)), 97.9 (d, 2 C, J = 155.9 Hz, C(3)), 52.6 (t, 4 C, J = 156.6 Hz, C(1,5)), 28.5 (q, 4 C, J = 126.6 Hz, CH_3–PD), 18.2 (q of d, 2 C, J = 137.2, 14.5 Hz, PCH_3). ^{31}P NMR (benzene-d_6, ambient): δ 18.65 (s). Anal. Calcd for $C_{22}H_{33}PZr$: C, 62.76; H, 7.93. Found: C, 62.46; H, 8.22.

$Zr(2,4\text{-}C_7H_{11})_2P(CH_3)_3$. The preparation of the trimethylphosphine adduct is done in an exactly analogous manner by substituting trimethylphosphine for the dimethylphenylphosphine. Thus, a solution of 4.38 g (32.6 mmol) of potassium 2,4-dimethylpentadienide in 50 mL of THF is added to a mixture of 3.00 g (7.95 mmol) of $ZrCl_4(THF)_2$ and 1.17 mL (7.95 mmol) of trimethylphosphine in 50 mL of THF at −78 °C, resulting in a red solution. The product is isolated as dark green crystals (mp 171–172 °C dec) in 78% yield (2.2 g, 6.2 mmol) by following the procedure identical to that reported for the dimethylphenylphosphine analog. The complexes are equally air-sensitive, smoldering upon exposure to air, although the trimethylphosphine adduct is slightly less soluble in hydrocarbon solvents.

^1H NMR (benzene-d_6, ambient): δ 4.48 (s, 2 H, H(3)), 2.65 (d, 4 H, J = 2.3 Hz, H(1,5exo)), 1.70 (s, 12 H, CH_3–PD), 1.45 (d, 9 H, J = 5.7 Hz, PCH_3), 0.34 (t, 4 H, J = 5.1 Hz, H(1,5endo)). ^{13}C NMR (benzene-d_6, ambient): δ 115.8 (s, 4 C, C(2,4)), 98.3 (d, 2 C, J = 157.8 Hz, C(3)), 51.4 (t, 4 C, J = 151.9 Hz, C(1,5)), 28.8 (q, 4 C, J = 126.7 Hz, CH_3–PD), 19.7 (q of d, 3 C, J = 128.1 Hz, 14.9 Hz, PCH_3). ^{31}P NMR (benzene-d_6, ambient): δ 0.03 (s). Anal. Calcd for $C_{17}H_{31}PZr$: C, 57.09; H, 8.74. Found: C, 57.54; H, 8.82.

$Zr(2,4\text{-}C_7H_{11})_2P(OCH_2)_3CCH_3$. A 100-mL, two-neck flask equipped with a magnetic stirring bar and nitrogen inlet is charged with 0.60 g (1.5 mmol) of $Zr(2,4\text{-}C_7H_{11})_2P(C_2H_5)_3$ and 0.25 g (1.7 mmol) of the "caged phosphite", $P(OCH_2)_3CCH_3$ (*Caution*! toxic), and removed from the drybox. THF (30 mL) is added via syringe, and the resulting dark green solution is stirred at room temperature for 1 h, at the end of which time the solvent is removed in vacuo. The dark green residue is extracted with 40 mL of toluene and filtered through a Celite pad, and the filtrate is then concentrated in vacuo to ca. 25 mL. Cooling of the filtrate at −20 °C overnight results in 0.64 g of a green, microcrystalline product (mp 124–126 °C dec) that is isolated and dried in vacuo. The microcrystalline sample is subsequently shown to be analytically pure $Zr(2,4\text{-}C_7H_{11})_2(P(OCH_2)_3CCH_3)$, isolated in quantitative yield from the triethylphosphine adduct.

^1H NMR (toluene-d_8, ambient): δ 4.71 (s, 2 H, H(3)), 3.64 (d, 6 H, J = 3.9 Hz, $P(OCH_2)$), 3.07 (s, 4 H, H(1,5exo)), 1.70 (s, 12 H, CH_3–PD), 0.84 (t, 4 H, J = 6.5 Hz, H(1,5endo)), −0.17 (d, 3 H, J = 9.5 Hz, $P(OCH_2)_3CCH_3$). ^{13}C NMR (toluene-d_8, ambient): δ 117.9 (s, 4 C, C(2,4)), 100.4 (d, 2 C, J = 156.3 Hz, C(3)), 74.9 (t of d, 3 C, J = 148.1, J_{P-C} = 14.3 Hz, $P(OCH_2)_3CCH_3$), 54.8 (t, 4 C, J = 158.9 Hz, C(1,5)), 31.6 (s, 1 C, $P(OCH_2)_3CCH_3$), 27.3 (q, 4 C, J = 127.4 Hz, CH_3–PD), 14.9 (q, 1 C, J = 127.5 Hz, $P(OCH_2)_3CCH_3$). Anal. Calcd for $C_{19}H_{31}O_3PZr$: C, 53.11; H, 7.27. Found: C, 52.83; H, 7.46.

$Zr(2,4\text{-}C_7H_{11})_2(CO)_2$. A 250-mL, two-neck flask equipped with a gas inlet and magnetic stirring bar is charged with 1.50 g (3.57 mmol) of $Zr(2,4\text{-}C_7H_{11})_2(P(CH_3)_2(C_6H_5))$ and placed under a carbon monoxide atmosphere; pentane (50 mL) is added via syringe and rapid stirring initiated. The solution rapidly (ca. 5–10 s) turns from green to blood red and carbon monoxide is steadily absorbed, as evidenced by a bubbler. The consumption of carbon monoxide continues at a rapid pace for several minutes and then gradually slows to a stop over the next hour. The now deep red solution is cooled to −78 °C in a dry ice–2-propanol bath, with care being taken to ensure that a partial vacuum is not created upon cooling. During this time a jacketed Schlenk frit packed with a 1-cm silica pad is evacuated, placed under a carbon monoxide atmosphere, and cooled to −78 °C in preparation for the ensuing filtration. A stainless steel cannula (16 gauge) is used to transfer the reaction mixture under carbon monoxide into the precooled frit, and application of a partial vacuum to the receiving flask results in a rapid filtration of the reaction mixture through the silica pad. Following removal of the frit from the receiving flask, the bright red filtrate is allowed to warm to ambient temperature under a carbon monoxide atmosphere and concentration of the filtrate to ca. 15 mL is achieved by evaporation with a stream of carbon monoxide gas over the surface of the solution. The concentrated solution is cooled to −78 °C while ca. 1 atm of CO pressure is maintained in the flask. Subsequently, the flask is placed into a −80 °C freezer for 2 days, during which time deep red cubes of the product are formed. The supernatant is removed via syringe and the crystals are dried with a stream of carbon monoxide, resulting in 0.55 g (46% yield) of highly air-sensitive red cubes (mp 65–68 °C). The dicarbonyl complex, $Zr(2,4\text{-}C_7H_{11})_2(CO)_2$, may be handled under a nitrogen atmosphere for periods of up to 1 h without decomposition in the solid state, whereas solutions of the product readily turn green in the absence of CO.

^1H NMR (toluene-d_8, −80 °C): δ 4.75 (s, 1 H, H(3)), 4.59 (s, 1 H, H(3)), 3.53 (s, 1 H, H(1,5exo)), 3.44 (s, 1 H, H(1,5exo)), 2.33 (s, 1 H, H(1,5exo)), 2.12 (s, 1 H, H(1,5exo)), 1.91 (s, 3 H, CH_3), 1.71 (s, 3 H, CH_3), 1.70 (s, 3 H, CH_3), 1.67 (s, 3 H, CH_3), 1.42 (s, 1 H, H(1,5endo)), 0.82 (s, 1 H, H(1,5endo)), 0.19 (s, 1 H, H(1,5endo)), −0.14 (s, 1 H, H(1,5endo)). ^{13}C NMR (toluene-d_8, −80 °C): δ 229.3 (s, 1 C, CO), 223.9 (s, 1 C, CO), 122.4 (s, 1 C, C(2 or 4)), 118.9 (s, 1 C, C(2 or 4)), 115.9 (s, 1 C, C(2 or 4)), 112.4 (s, 1 C, C(2 or 4)), 101.8 (d, 1 C, J = 160.4 Hz, C(3)), 91.1 (d, 1 C, J = 159.9 Hz, C(3)), 74.7 (t, 1 C, J = 157.0 Hz, C(1 or 5)), 65.1 (t, 1 C, J = 157.7 Hz, C(1 or 5)), 63.4 (t, 1 C, J = 157.7 Hz, C(1 or 5)), 53.7 (t, 1 C, J = 153.2 Hz, C(1 or 5)), 30.0 (q, 1 C, J = 126.8 Hz, CH_3), 29.6 (q, 1 C, J = 127.2 Hz, CH_3), 28.4 (q, 1 C, J = 127.5 Hz, CH_3), 28.3 (q, 1 C, J = 126.9 Hz, CH_3). IR (pentane solution): 2000 (vs, sh), 1942 (vs, sh) cm^{-1}. Anal. Calcd for $C_{16}H_{22}O_2Zr$: C, 56.83; H, 6.57. Found: C, 56.44; H, 6.80.

Zr(2,4-C_7H_{11})$_2$CO. Into a 250-mL, two-neck round-bottom flask, equipped with a nitrogen inlet and magnetic stirring bar is placed 0.51 g (1.5 mmol) of Zr(2,4-C_7H_{11})$_2$(CO)$_2$, after which the flask is removed from the drybox. Hexanes (50 mL) are added via syringe, and the resulting blood red solution is placed under a static vacuum while being stirred rapidly. Vigorous stirring is continued for 3 h, during which time the color of the solution steadily turns from red to dark green, indicating the formation of the monocarbonyl complex. A solution IR spectrum at the end of this period indicates only peaks corresponding to the monocarbonyl complex, and following concentration of the solution in vacuo to ca. 10 mL and cooling to −30 °C for 12 h, green-black rods of the product are formed. The supernatant was removed via syringe and the product dried in vacuo to yield 0.42 g (92% yield) of dark green pyrophoric crystals (mp 77–79 °C dec).

^{1}H NMR (benzene-d_6, ambient): δ 4.65 (s, 2 H, H(3)), 3.05 (s, 4 H, H(1,5exo)), 1.46 (s, 12 H, CH_3–Pdl), 0.48 (s, 4 H, H(1,5endo)). ^{13}C NMR (benzene-d_6, ambient): δ 246.8 (s, 1 C, CO), 116.3 (s, 4 C, C(2,4)), 98.8 (d, 2 C, J = 157.8 Hz, C(3)), 54.8 (t, 4 C, J = 154.6 Hz, C(1,5)), 27.9 (q, 4 C, J = 127.3 Hz, CH_3–Pdl). Anal. Calcd for $C_{15}H_{22}OZr$: C, 58.20; H, 7.16. Found: C, 57.17; H, 7.33.

Hf(2,4-C_7H_{11})$_2$P(C_2H_5)$_3$. In a 250 mL, three-neck flask equipped with a magnetic stirring bar, nitrogen inlet, and pressure-equalizing funnel, 1.84 g (1.77 mmol) of [HfCl$_3$(P(C_2H_5)$_3$)$_2$]$_2$[9] is dissolved in 50 mL of THF to give an almost colorless solution. The flask is cooled to −78 °C, and a solution of 1.50 g (11.2 mmol) of potassium 2,4-dimethylpentadienide in 50 mL of THF is added dropwise to the stirred solution. The reaction mixture is initially yellow but turns yellow-green on warming and finally becomes a deep green-black. After reaching room temperature, the solution is stirred for an additional 8 h. Following THF removal under reduced pressure, a sticky green-black residue remains. Extraction of this residue with 200 mL of pentane gives a blackish solution which is filtered through Celite on a coarse frit and concentrated to 20 mL in vacuo. After 3 days at −20 °C, 153 mg (0.314 mmol) of (triethylphosphine)bis(2,4-dimethylpentadienyl)hafnium is isolated as black crystals (mp 140–141 °C). The yield is 8.9% based on "[HfCl$_3$(P(C_2H_5)$_3$)$_2$]$_2$".

^{1}H NMR (benzene-d_6, ambient): δ 4.38 (s, 2 H, H(3)), 2.38 (s, 4 H, H_x(1,5)), 1.88 (s, 12 H, CH_3), 1.51 (m, 6 H, P*CH*$_2$CH$_3$), 0.99 (m, 9 H, PCH$_2$*CH*$_3$), 0.14 (apparent t, 4 H, J = 6 Hz, H_n(1,5)). ^{13}C{^{1}H} NMR (benzene-d_6, ambient): δ 112.9 (s), 97.9 (d), 48.2 (t), 28.8 (q), 17.7 (t), 7.6 (q). Anal. Calcd for $C_{20}H_{37}PHf$: C, 49.33; H, 7.66. Found: C, 49.38; H, 7.67.

Hf(2,4-C_7H_{11})$_2$(P(CH_3)$_2$(C_6H_5)). Freshly sublimed HfCl$_4$ (0.71 g, 2.2 mmol) is placed in a three-neck flask equipped with a nitrogen inlet, magnetic stirring bar, and pressure-equalizing dropping funnel and removed from the drybox. Toluene (30 mL) and dimethylphenylphosphine (0.63 mL, 4.4 mmol) are added via syringe, the resulting pale yellow heterogeneous mixture is cooled to −78 °C, and potassium 2,4-dimethylpentadienide (1.22 g, 9.08 mmol) in 10 mL of THF is added dropwise. The now red reaction mixture is stirred for 30 min at −78 °C and then warmed to ambient temperature and stirred for an additional 90 min, during which time the color darkens to red-brown. At the end of this period the solvent is removed in vacuo and the resulting dark brown solid extracted with four 50-mL portions of diethyl ether. Filtration of the ether extracts through a Celite pad on a coarse frit followed by concentration of the red-brown filtrate to ca. 100 mL and cooling at −30 °C for 24 h results in the formation of metallic red-black needles of the product. The supernatant is transferred via syringe to a clean flask, and the crystals are dried under vacuum. The supernatant is further concentrated to ca. 45 mL and cooled at −30 °C for 2 days, resulting in the isolation of a second crop of crystals for an overall yield of 31% (0.35 g). The crystals (mp 160–161 °C dec) are extremely air-sensitive, often smoldering upon exposure to the atmosphere, and smell quite strongly of dimethylphenylphosphine.

^{1}H NMR (benzene-d_6, ambient): δ 7.36–7.12 (m, 5 H, Ph), 4.40 (s, 2 H, H(3)), 2.26 (s, 4 H, H(1,5exo)), 1.80 (s, 12 H, CH_3–PD), 1.57 (d, 6 H, J = 6 Hz, P*CH*$_3$), −0.15 (t, 4 H, J = 9.0 Hz, H(1,5endo)). ^{13}C NMR (benzene-d_6, ambient): δ 128.7–127.6 (m, 6 C, P*Ph*), 113.4 (s, 4 C, C(2,4)), 99.3 (d, 2 C, J = 155.8 Hz, C(3)), 49.9 (t, 4 C, J = 149.9 Hz, C(1,5)), 29.2 (q, 4 C, J = 126.8 Hz, CH_3–PD), 18.6 (q of d, 2 C, 126.5, 16.0 Hz, P*CH*$_3$). ^{31}P NMR (benzene-d_6, ambient): δ 7.39 (s). Anal. Calcd for $C_{22}H_{33}HfP$: C, 52.02; H, 6.56. Found: C, 52.61; H, 6.37.

Hf(2,4-C_7H_{11})$_2$(CO)$_2$. The hafnium dicarbonyl complex is prepared from the dimethylphenylphosphine adduct, Hf(2,4-C_7H_{11})$_2$(P(CH_3)$_2$(C_6H_5)), and CO in a fashion similar to that of the zirconium analog. Subsequently, a low-temperature filtration of the impure reaction mixture of 0.75 g (1.5 mmol) of Hf(2,4-C_7H_{11})$_2$P(CH_3)$_2$(C_6H_5) in 50 mL of pentane under carbon monoxide results in a bright red filtrate from which deep red crystals (0.34 g, 55% yield, mp 62–63 °C dec) of the title complex can be isolated. The crystallization techniques are exactly analogous to those used for the zirconium analog. Bis(2,4-dimethylpentadienyl)hafnium dicarbonyl forms deep red highly air-sensitive cubes which decompose over a period of several weeks upon standing at ambient temperature under a carbon monoxide atmosphere.

^{1}H NMR (toluene-d_8, −90 °C): δ 4.71 (s, 1 H, H(3)), 4.66 (s, 1 H, H(3)), 3.50 (s, 1 H, H(1,5exo)), 3.41 (s, 1 H, H(1,5exo)), 2.27 (s, 1 H, H(1,5exo)), 2.02 (s, 1 H, H(1,5exo)), 2.12 (s, 3 H, CH_3), 1.91 (s, 6 H, CH_3), 1.84 (s, 3 H, CH_3), 1.32 (s, 1 H, H(1,5endo)), 0.73 (s, 1 H, H(1,5endo)), 0.06 (s, 1 H, H(1,5endo)), −0.34 (s, 1 H, H(1,5endo)). ^{13}C NMR (toluene-d_8, −80 °C): δ 225.3 (s, 1 C, CO), 220.9 (s, 1 C, CO), 121.0 (s, 1 C, C(2 or 4)), 116.1 (s, 1 C, C(2 or 4)), 112.1 (s, 1 C, C(2 or 4)), 109.8 (s, 1 C, C(2 or 4)), 102.7 (d, 1 C, J = 161.4 Hz, C(3)), 92.4 (d, 1 C, J = 163.9 Hz, C(3)), 71.9 (t, 1 C, J = 159.4 Hz, C(1 or 5)), 60.9 (t, 1 C, J = 153.7 Hz, C(1 or 5)), 59.3 (t, 1 C, J = 156.0 Hz, C(1 or 5)), 50.5 (t, 1 C, J = 151.3 Hz, C(1 or 5)), 29.7 (q, 1 C, J = 129.6 Hz, CH_3), 29.6 (q, 1 C, J = 129.6 Hz, CH_3), 28.0 (q, 1 C, J = 127.5 Hz, CH_3), 27.9 (q, 1 C, J = 127.9 Hz, CH_3). IR (pentane solution): 1990 (vs, sh), 1932 (vs, sh) cm^{-1}. Anal. Calcd for $C_{16}H_{22}HfO_2$: C, 45.23; H, 5.22. Found: C, 46.30; H, 5.44.

Nb(2,4-C_7H_{11})$_2$P(C_2H_5)$_3$. A 250 mL, three-neck flask equipped with a nitrogen inlet, a magnetic stirring bar, and a dropping funnel is charged with 0.38 g (1.0 mmol) of light yellow NbCl$_4$(THF)$_2$[10] and 40 mL of THF. By syringe, 0.37 mL (2.5 mmol) of triethylphosphine is added to the stirred suspension. The solid material dissolves rapidly to give a yellow-orange solution of trans-NbCl$_4$(P(C_2H_5)$_3$)$_2$.[11] After the flask is cooled to −78 °C, a solution of 0.54 g (4.0 mmol) of potassium 2,4-dimethylpentadienide in 50 mL of THF is added dropwise to the niobium compound. The reaction mixture is initially orange but turns brown on warming. When the temperature has reached −20 °C, the solution turns dark green and stays that color. Upon reaching room temperature, the solution is stirred for an additional 4–6

---

[9] (a) Morse, P. M.; Wilson, S. R.; Girolami, G. S. *Inorg. Chem.* **1990**, *29*, 3200. (b) Wengrovius, J. H.; Schrock, R. R.; Day, C. S. *Ibid.* **1981**, *20*, 1844.

[10] Manzer, L. E. *Inorg. Chem.* **1977**, *16*, 525.

[11] Cotton, F. A.; Duraj, S. A.; Roth, W. J. *Inorg. Chem.* **1984**, *23*, 3592.

Table I. X-ray Data Collection Parameters for Zr(2,4-C_7H_{11})$_2$(PEt$_3$) (A), Nb(2,4-C_7H_{11})$_2$(PEt$_3$) (B), Zr(2,4-C_7H_{11})$_2$CO (C), Zr(2,4-C_7H_{11})$_2$(CO)$_2$ (D), and Mo(2,4-C_7H_{12})$_2$(PEt$_3$)

	A	B	C	D	E
formula	$C_{20}H_{37}PZr$	$C_{20}H_{37}PNb$	$C_{15}H_{22}OZr$	$C_{16}H_{22}O_2Zr$	$C_{20}H_{37}PMo$
mol wt	399.71	401.40	309.56	337.57	404.43
space group	$P\bar{1}$	$P\bar{1}$	$P2_12_12_1$	$P\bar{1}$	Pbca
a, Å	7.988(4)	7.936(2)	11.827(2)	8.552(3)	11.244(2)
b, Å	8.631(4)	8.735(2)	12.158(2)	9.243(3)	14.516(2)
c, Å	15.649(7)	15.511(5)	10.328(2)	20.419(8)	24.963(4)
α, deg	87.98(4)	87.82(2)	90	93.34(3)	90
β, deg	103.46(4)	103.79(2)	90	83.88(3)	90
γ, deg	91.70(4)	91.12(2)	90	87.97(3)	90
d_{calc}, g/cm^3	1.27	1.28	1.38	1.40	1.32
λ	0.710 73	0.710 73	0.710 73	0.710 73	0.710 73
temp, °C	20	20	16	16	20
cryst size, mm	0.30 × 0.25 × 0.45	0.20 × 0.22 × 0.36	0.35 × 0.32 × 0.30	0.40 × 0.30 × 0.18	0.18 × 0.22 × 0.35
linear abs coeff, cm^{-1}	5.60	5.97	7.12	6.71	6.11
scan type	ω	θ–2θ	θ–2θ	θ–2θ	θ–2θ
scan speed, deg/min	2–24	2–24	2–8	2.5–8	2–24
abs treatment	none	numerical	none	scan	none
rel trans factors		0.83–0.90		0.81–1.00	
scan range, deg	1	±1	±1	±1	±1
2θ limits, deg	3–60	3.5–50	3–49	2.5–48	3–50
min *hkl*	–11,–12,0	–9,–10,0	000	0,–10,–23	000
max *hkl*	11,12,22	9,10,18	13,14,12	9,10,23	13,17,29
no. of unique, obsd data	4692 (2.5σ)	2593 (2.5σ)	1266 (3σ)	3229 (3σ)	1803 (3σ)
no. of variables	199	199	155	347	199
$R(F)$	0.081	0.051	0.032	0.036	0.080
$R_w(F)$	0.097	0.052	0.036	0.040	0.097
max diff Fourier peak, e/Å^3	1.10	0.62	0.36	0.71	0.93

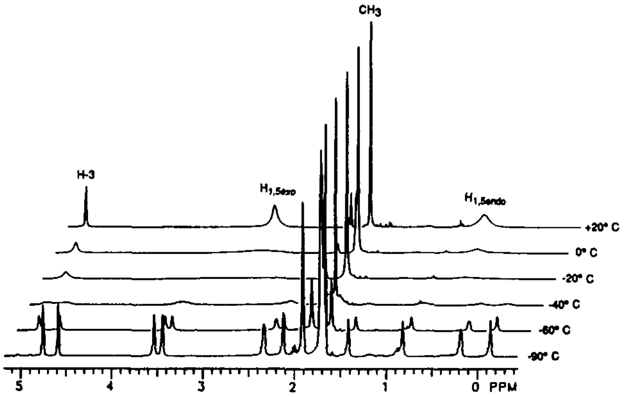

Figure 1. Representative variable-temperature ^{1}H NMR spectra for Zr(2,4-C_7H_{11})$_2$(CO)$_2$.

h. The THF is removed under reduced pressure, and the green-brown solid which remains is extracted with several 50-mL portions of pentane. The green pentane solution is filtered through a pad of Celite on a coarse frit and reduced in volume to 30 mL. Cooling the flask to –20 °C for 2 days yields 160 mg (0.40 mmol) of dark green crystals (mp 146–147 °C). The yield is 40% based on NbCl$_4$(THF)$_2$. The reaction may also be carried out with the addition of only 1 equiv of PEt$_3$.

ESR (1 × 10^{-3} M toluene solution): g = 1.989, A_v = 120.6 G. Magnetic susceptibility (THF solution, Evans' method): μ = 1.61 μ_B. Anal. Calcd for $C_{20}H_{37}PNb$: C, 59.85; H, 7.29. Found: C, 59.53; H, 7.78.

Mo(2,4-C_7H_{11})$_2$P(C_2H_5)$_3$. The MoCl$_4$(THF)$_2$ used in this synthesis is prepared by a published procedure.[12] It should be used within 2–3 weeks of preparation, while it is still orange. Orange-brown or brown MoCl$_4$(THF)$_2$ gives lower yields.

A 250-mL, three-neck flask equipped with a nitrogen inlet, magnetic stirring bar, and dropping funnel is charged with 0.38 g (1.0 mmol) of orange, microcrystalline MoCl$_4$(THF)$_2$ and 50 mL of THF. To the stirred suspension is added by syringe 0.30 mL (2.0 mmol) of triethylphosphine, resulting in a rapid dissolution of the solid to give a dark red solution. The flask is cooled to –78 °C, and a solution of 0.55 g (4.0 mmol) of potassium 2,4-dimethylpentadienide in 50 mL of THF is added dropwise. After approximately one-third of the potassium salt has been added, the solution turns green but becomes greenish-yellow after the addition is complete. Upon reaching room temperature, the reaction mixture is stirred for an additional 6–8 h. The THF is removed in vacuo from the now orange-yellow solution to give an orange-brown residue. The solid is extracted with two 25-mL portions of pentane, and the yellow pentane solution is filtered through a Celite pad. Following reduction of the solution volume to about 5 mL, the flask is placed in a –20 °C freezer. In the absence of seed crystals the time for crystallization to occur is somewhat unpredictable, sometimes taking weeks. If, however, seed crystals are added to the cold, concentrated solution, X-ray-quality crystals can be grown in 2–3 days at –20 °C. In this manner 305 mg (0.754 mmol) of lemon yellow, rod-shaped crystals of the title compound are isolated (mp 103–104 °C). This corresponds to a 75.4% yield based on MoCl$_4$(THF)$_2$.

Table II. Positional Parameters for the Non-Hydrogen Atoms of Zr(2,4-C_7H_{11})$_2$(PEt$_3$)

atom	*x*	*y*	*z*
Zr	0.16252(7)	0.15810(7)	0.28934(4)
C(1)	0.4238(11)	0.2920(11)	0.3754(5)
C(2)	0.3388(10)	0.2235(10)	0.4382(5)
C(3)	0.3082(10)	0.0666(9)	0.4399(5)
C(4)	0.3082(10)	–0.0555(9)	0.3850(5)
C(5)	0.3896(11)	–0.0471(11)	0.3140(6)
C(6)	0.2912(16)	0.3262(14)	0.5024(7)
C(7)	0.2302(14)	–0.2074(11)	0.4061(8)
C(8)	–0.0147(11)	0.3812(10)	0.2326(6)
C(9)	–0.0831(9)	0.3105(11)	0.2989(5)
C(10)	–0.1306(9)	0.1464(8)	0.3040(5)
C(11)	–0.1213(8)	0.0283(7)	0.2508(5)
C(12)	–0.0556(10)	0.0423(10)	0.1720(5)
C(13)	–0.1054(12)	0.4101(13)	0.3752(7)
C(14)	–0.1708(10)	–0.1306(11)	0.2794(7)
P	0.3063(2)	0.2348(2)	0.1517(1)
C(1A)	0.1596(13)	0.2983(12)	0.0488(6)
C(1B)	0.2357(17)	0.3428(16)	–0.0285(8)
C(2A)	0.4753(14)	0.3849(15)	0.1672(8)
C(2B)	0.4167(24)	0.5431(15)	0.1885(12)
C(3A)	0.4238(15)	0.0832(14)	0.1123(7)
C(3B)	0.3100(24)	–0.0559(15)	0.0740(8)

^{1}H NMR (benzene-d_6, ambient): δ 4.41 (s, 1 H), 2.45 (apparent t, 1 H, J = 2 Hz), 2.34 (apparent t, 1 H, J = 3 Hz), 2.10 (s, 1 H),

---

[12] Anker, M. W.; Chatt, J.; Leigh, G. J.; Wedd, A. G. *J. Chem. Soc., Dalton Trans.* 1975, 2639.

Table III. Selected Bond Distances (Å) and Angles (deg) for $Zr(2,4-C_7H_{11})_2(PEt_3)$

Bond Distances

Zr–C(1)	2.483(8)	Zr–C(8)	2.441(9)	C(1)–C(2)	1.422(13)	C(8)–C(9)	1.395(13)
Zr–C(2)	2.499(7)	Zr–C(9)	2.430(8)	C(2)–C(3)	1.403(12)	C(9)–C(10)	1.460(11)
Zr–C(3)	2.447(7)	Zr–C(10)	2.404(7)	C(3)–C(4)	1.420(12)	C(10)–C(11)	1.353(11)
Zr–C(4)	2.473(8)	Zr–C(11)	2.454(6)	C(4)–C(5)	1.411(13)	C(11)–C(12)	1.448(12)
Zr–C(5)	2.529(9)	Zr–C(12)	2.438(7)	C(2)–C(6)	1.483(15)	C(9)–C(13)	1.541(15)
P–C(1A)	1.835(9)	Zr–P	2.721(2)	C(4)–C(7)	1.494(13)	C(11)–C(14)	1.499(12)
P–C(2A)	1.824(12)	C(1A)–C(1B)	1.507(17)	C(2A)–C(2B)	1.529(20)	C(3A)–C(3B)	1.536(18)
P–C(3A)	1.836(13)						

Bond Angles

C(1)–C(2)–C(3)	124.1(8)	C(3)–C(4)–C(7)	114.3(8)	C(10)–C(9)–C(13)	116.4(8)
C(1)–C(2)–C(6)	117.9(8)	C(5)–C(4)–C(7)	118.3(8)	C(10)–C(11)–C(12)	124.9(7)
C(2)–C(3)–C(4)	130.3(8)	C(8)–C(9)–C(10)	125.2(8)	C(10)–C(11)–C(14)	117.2(8)
C(3)–C(2)–C(6)	117.9(8)	C(8)–C(9)–C(13)	118.4(8)	C(12)–C(11)–C(14)	117.7(7)
C(3)–C(4)–C(5)	127.4(8)	C(9)–C(10)–C(11)	131.3(8)	Zr–P–C(1A)	116.9(4)
P–C(1A)–C(1B)	118.1(8)	P–C(3A)–C(3B)	113.8(10)	Zr–P–C(2A)	118.1(4)
P–C(2A)–C(2B)	113.9(10)			Zr–P–C(3A)	117.2(4)

Table IV. Positional Parameters for the Non-Hydrogen Atoms of $Nb(2,4-C_7H_{11})_2(PEt_3)$

atom	*x*	*y*	*z*
Nb	0.16566(7)	0.16093(6)	0.28935(4)
C(1)	0.4246(9)	0.2923(9)	0.3732(5)
C(2)	0.3343(9)	0.2301(8)	0.4350(4)
C(3)	0.2811(9)	0.0741(8)	0.4386(4)
C(4)	0.3013(9)	–0.0478(8)	0.3854(4)
C(5)	0.3850(10)	–0.0335(9)	0.3139(5)
C(6)	0.2902(12)	0.3340(10)	0.5024(5)
C(7)	0.2238(12)	–0.2011(9)	0.4048(6)
C(8)	–0.0079(10)	0.3733(8)	0.2310(5)
C(9)	–0.0736(8)	0.3076(8)	0.3020(4)
C(10)	–0.1239(8)	0.1496(7)	0.3081(4)
C(11)	–0.1087(8)	0.0294(7)	0.2527(5)
C(12)	–0.0495(9)	0.0501(8)	0.1722(4)
C(13)	–0.0950(11)	0.4115(9)	0.3753(6)
C(14)	–0.1643(11)	–0.1316(9)	0.2787(6)
P	0.3044(2)	0.2381(2)	0.1555(1)
C(3A)	0.4267(11)	0.0926(9)	0.1157(5)
C(3B)	0.3196(16)	–0.0484(10)	0.0768(6)
C(1A)	0.1533(11)	0.3008(10)	0.0497(5)
C(1B)	0.2310(14)	0.3473(12)	–0.0292(5)
C(2A)	0.4726(12)	0.3941(10)	0.1721(6)
C(2B)	0.4076(19)	0.5510(11)	0.1863(8)

2.09 (hidden d, 1 H, *J* = 4 Hz), 1.95 (s, 3 H), 1.71 (d, 1 H, *J* = 7 Hz), 1.65 (s, 1 H), 1.61 (s, 3 H), 1.60 (s, 3 H), 1.59 (s, 3 H), 1.41 (m, 6 H, PCH_2CH_3), 0.87 (obscured d, 1 H, *J* = 6 Hz), 0.84 (m, 9 H, PCH_2CH_3), 0.08 (dd, 1 H, *J* = 8 Hz, *J* = 4 Hz), –0.63 (dd, 1 H, *J* = 7, 2 Hz). $^1H\{^{31}P\}$ NMR (benzene-d_6, ambient): δ 4.41 (s, 1 H), 2.43 (s, 1 H), 2.33 (d, 1 H, *J* = 3.8 Hz), 2.08 (s, 2 H), 1.94 (s, 3 H), 1.70 (s, 1 H), 1.64 (s, 1 H), 1.61 (s, 3 H), 1.60 (s, 3 H), 1.58 (s, 3 H), 1.41 (m, 6 H, PCH_2CH_3), 0.87 (obscured s, 1 H), 0.85 (m, 9 H, PCH_2CH_3), 0.08 (d, 1 H, *J* = 3.8 Hz), –0.66 (d, 1 H, *J* = 2 Hz). ^{13}C NMR (benzene-d_6, ambient): δ 119.7 (s), 101.6 (d, *J* = 155 Hz), 101.1 (s), 96.4 (s), 76.2 (s), 72.7 (d, *J* = 166 Hz), 48.9 (t, *J* = 145 Hz), 48.4 (t, *J* = 154 Hz), 44.4 (t, *J* = 149 Hz), 43.1 (t, *J* = 150 Hz), 26.5 (q, *J* = 128 Hz), 24.9 (q, *J* = 126 Hz), 24.1 (q, *J* = 125 Hz), 17.5 (td, J_{C-H} = 125 Hz, J_{C-P} = 20 Hz), 15.7 (q, *J* = 127 Hz), 7.6 (q, *J* = 126 Hz). $^{31}P\{^1H\}$ NMR (benzene-d_6, ambient): δ 33.7. Anal. Calcd for $C_{20}H_{37}PMo$: C, 59.40; H, 9.22. Found: C, 59.89; H, 9.53.

X-ray Structural Studies. Single crystals of the various compounds were prepared by the slow cooling of their concentrated solutions, utilizing the solvents mentioned for their extractions. Data were collected with a Nicolet-Siemens P$\bar{1}$ autodiffractometer. The metal atom positions for the phosphine complexes were determined from a Patterson map, while those for the carbonyl complexes were obtained by direct methods. Subsequently, the remaining non-hydrogen atom positions were found from a combination of difference Fourier maps and least-squares refinements for which the function $\sum w(|F_o| - |F_c|)$ was minimized. Nearly all hydrogen atoms could be located, and they are included in fixed, idealized positions. All refinements proceeded routinely. Pertinent parameters related to the data collection and refinement are presented in Table I.

Synthetic Results and Discussion

The reactions of various $MCl_4(PR_3)_2$ complexes with 4 equiv of $K(2,4-C_7H_{11})$ (C_7H_{11} = dimethylpentadienyl) lead to the spontaneous reduction of the M(IV) species and formation of the respective open metallocene complex, $M(2,4-C_7H_{11})_2(PR_3)$ (eq 1). An alternate procedure could

$$MCl_4(L)_2 + 4K(2,4-C_7H_{11}) \rightarrow M(2,4-C_7H_{11})_2(L) \qquad (1)$$

$$M = Zr, Nb, Mo; L = PEt_3$$

$$M = Zr, Hf; L = PMe_2(C_6H_5)$$

$$M = Zr; L = PMe_3$$

$$(1/2)[MCl_3(PEt_3)_2]_2 + 3K(2,4-C_7H_{11}) \rightarrow M(2,4-C_7H_{11})_2(PEt_3) \qquad (2)$$

$$M = Zr, Hf$$

also be employed for hafnium and zirconium (eq 2) but generally was found less convenient. Except for the molybdenum complex, the phosphine ligands in these species are quite labile and readily replaced by smaller phosphines or phosphites, as in eq 3. For the zirconium

$$Zr(2,4-C_7H_{11})_2(PEt_3) + L \rightarrow Zr(2,4-C_7H_{11})_2(L) \qquad (3)$$

$$L = PMe_3, P(OMe)_3, P(OCH_2)_3CMe$$

$$M(2,4-C_7H_{11})_2PMe_2(C_6H_5) + 2CO \rightarrow M(2,4-C_7H_{11})_2(CO)_2 \qquad (4)$$

and hafnium complexes, the phosphine ligands could also be replaced by CO, leading to 18-electron dicarbonyl complexes (eq 4), the first examples in which two additional ligands could be added to an open metallocene.[13] For the

---

[13] We have also found it possible to prepare $Zr(C_5H_7)_2(dmpe)$. Additionally, the fact that green, crystalline $Zr(2,4-C_7H_{11})_2(L)$ (L = PMe_3, $PMe_2C_6H_5$) are isolated from red solutions (see Experimental Section) might be an indication that bis(phosphine) complexes are present in solution. An apparent ^{31}P NMR signal in CO + $Zr(2,4-C_7H_{11})_2(PEt_3)$ mixtures (δ –18.9) might also be indicative of a mixed CO/PEt_3 complex.

Table V. Selected Bond Distances (Å) and Angles (deg) for $Nb(2,4\text{-}C_7H_{11})_2(PEt_3)$

Bond Distances

Nb–C(1)	2.428(7)	Nb–C(8)	2.372(7)	C(1)–C(2)	1.410(11)	C(8)–C(9)	1.421(11)
Nb–C(2)	2.421(6)	Nb–C(9)	2.380(7)	C(2)–C(3)	1.414(10)	C(9)–C(10)	1.429(9)
Nb–C(3)	2.384(6)	Nb–C(10)	2.382(7)	C(3)–C(4)	1.409(10)	C(10)–C(11)	1.408(10)
Nb–C(4)	2.424(6)	Nb–C(11)	2.379(6)	C(4)–C(5)	1.422(11)	C(11)–C(12)	1.438(11)
Nb–C(5)	2.432(8)	Nb–C(12)	2.385(6)	C(2)–C(6)	1.520(12)	C(9)–C(13)	1.525(11)
P–C(1A)	1.863(7)	Nb–P	2.628(2)	C(4)–C(7)	1.502(11)	C(11)–C(14)	1.527(10)
P–C(2A)	1.853(9)	C(1A)–C(1B)	1.528(13)	C(2A)–C(2B)	1.524(15)	C(3A)–C(3B)	1.528(12)
P–C(3A)	1.838(9)								

Bond Angles

C(1)–C(2)–C(3)	123.7(7)	C(3)–C(4)–C(7)	117.0(7)	C(10)–C(9)–C(13)	117.9(6)
C(1)–C(2)–C(6)	119.3(7)	C(5)–C(4)–C(7)	118.7(7)	C(10)–C(11)–C(12)	124.0(6)
C(2)–C(3)–C(4)	130.1(7)	C(8)–C(9)–C(10)	123.7(7)	C(10)–C(11)–C(14)	117.6(7)
C(3)–C(2)–C(6)	117.0(7)	C(8)–C(9)–C(13)	118.4(6)	C(12)–C(11)–C(14)	118.4(6)
C(3)–C(4)–C(5)	124.3(6)	C(9)–C(10)–C(11)	129.1(7)	Nb–P–C(1A)	116.9(3)
P–C(1A)–C(1B)	118.2(6)	P–C(3A)–C(3B)	115.0(7)	Nb–P–C(2A)	117.6(3)
P–C(2A)–C(2B)	114.7(8)			Nb–P–C(3A)	117.7(3)

more stable zirconium complex, one of the carbonyl ligands is readily lost when its solutions are placed under static vacuum, yielding the green monocarbonyl (eq 5).

$$Zr(2,4\text{-}C_7H_{11})_2(CO)_2 \rightleftharpoons Zr(2,4\text{-}C_7H_{11})_2(CO) + CO \quad (5)$$

NMR spectroscopic data for the diamagnetic, 16-electron $M(2,4\text{-}C_7H_{11})_2(L)$ (M = Zr, Hf) compounds are in accord with the expected syn-eclipsed structure (I) found

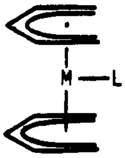

I

for related titanium analogs.[14] This has been confirmed by single-crystal X-ray structural analyses for $Zr(2,4\text{-}C_7H_{11})_2(L)$ (L = PEt_3, CO) and also for the paramagnetic, 17-electron $Nb(2,4\text{-}C_7H_{11})_2(PEt_3)$ (vide infra). However, NMR spectra for the 18-electron $Mo(2,4\text{-}C_7H_{11})_2(PEt_3)$ reveal a lack of any symmetry, and an entirely different structure has been found (vide infra).

For the $M(2,4\text{-}C_7H_{11})_2(CO)_2$ (M = Zr, Hf) compounds, more complex behavior was also found. While one can observe a four-line pattern in the ^1H NMR spectra at room temperature (Figure 1), some of the resonances are broad, and on cooling, eventually a 14-line pattern was found, indicating a lack of symmetry in the molecule. From a single-crystal structural analysis (vide infra), the structure was eventually found to be that of II, in which one carbonyl

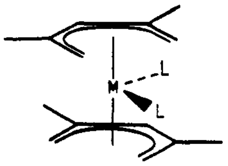

II

ligand is positioned by an open dienyl edge, the other by a central carbon atom of the second dienyl ligand. With

Table VI. Positional Parameters for the Non-Hydrogen Atoms of $Zr(2,4\text{-}C_7H_{11})_2(CO)$

atom	*x*	*y*	*z*
Zr	0.19879(5)	0.21479(5)	0.19496(6)
O	–0.0472(5)	0.1650(5)	0.3377(6)
C(1)	0.0788(6)	0.1900(7)	0.0012(7)
C(2)	0.1914(7)	0.1945(6)	–0.0404(6)
C(3)	0.2824(6)	0.1285(6)	0.0069(6)
C(4)	0.2790(6)	0.0446(5)	0.1068(7)
C(5)	0.1851(7)	0.0137(5)	0.1792(7)
C(6)	0.2243(7)	0.2830(8)	–0.1359(7)
C(7)	0.3953(7)	–0.0021(6)	0.1398(9)
C(8)	0.1349(7)	0.4028(6)	0.2543(8)
C(9)	0.2501(6)	0.4095(5)	0.2142(7)
C(10)	0.3416(6)	0.3463(6)	0.2628(6)
C(11)	0.3412(6)	0.2605(6)	0.3573(6)
C(12)	0.2488(6)	0.2271(7)	0.4281(6)
C(13)	0.2764(7)	0.4849(6)	0.1002(8)
C(14)	0.4519(7)	0.2011(8)	0.3726(7)
C(15)	0.0376(6)	0.1836(6)	0.2870(7)

this information, it becomes possible to interpret the variable-temperature NMR spectroscopic data. One can observe a clear coalescence of the two H(3) resonances (those most downfield), at ca. 245 K, which leads to the establishment of a C_2 axis of symmetry, rendering the two dienyl ligands equivalent. This can most readily be explained by a structure such as III, which has precedent in $Zr(C_5H_7)_2(dmpe)$[13] and various $M(allyl)_2(L)_2$ and $M(diene)_2(L)_2$ complexes.[15] Presumably, such a structure becomes destabilized here due to the presence of the methyl groups. In such a structure, however, the dienyl ligands themselves would not be symmetric (i.e., C(1) $\neq$ C(5); C(2) $\neq$ C(4)), and one should expect to see an intermediate seven-line ^1H NMR spectrum. That this pattern is not seen as an intermediate suggests that further oscillation of the two dienyl ligands occurs readily at that stage between the enantiomers III and IV. The barriers obtained for the establishment of the C_2 axis of symmetry are 12.0 ± 0.2 and 13.1 ± 0.2 kcal/mol for the respective zirconium and hafnium complexes.[16]

The C–O stretching frequencies for the $M(2,4\text{-}C_7H_{11})_2(CO)_2$ complexes are also of interest. For the zirconium complex the values are 1965 and 2000 cm^{-1}, whereas for hafnium they are 1932 and 1990 cm^{-1}. These values

---

[14] (a) Ernst, R. D. *Chem. Rev.* **1988**, *88*, 1255. (b) Ernst, R. D.; Freeman, J. W.; Stahl, L.; Wilson, D. R.; Ziegler, M. L. Manuscript in preparation.

[15] (a) Bleeke, J. R.; Hays, M. K. *Organometallics* **1984**, *3*, 506. (b) Marsh, R. A.; Hooward, J.; Woodward, P. *J. Chem. Soc., Dalton Trans.* **1973**, 778.

[16] (a) Kessler, H. *Angew. Chem.* **1970**, *9*, 219. (b) For the zirconium complex $\delta\nu$ = 50.1 Hz and T_c = 245 K. For the hafnium analog, these values are 15.2 Hz and 255 K, respectively. (c) Cotton, F. A.; Frenz, B. A. *Acta Crystallogr.* **1974**, *30B*, 1772.

Table VII. Pertinent Bond Distances (Å) and Angles (deg) for $Zr(2,4\text{-}C_7H_{11})_2(CO)$

Bond Distances

Zr–C(1)	2.472(7)	Zr–C(8)	2.484(8)	C(1)–C(2)	1.400(10)	C(8)–C(9)	1.426(10)
Zr–C(2)	2.445(6)	Zr–C(9)	2.451(6)	C(2)–C(3)	1.428(10)	C(9)–C(10)	1.419(9)
Zr–C(3)	2.419(6)	Zr–C(10)	2.429(6)	C(2)–C(6)	1.511(10)	C(9)–C(13)	1.524(10)
Zr–C(4)	2.452(6)	Zr–C(11)	2.441(6)	C(3)–C(4)	1.452(10)	C(10)–C(11)	1.429(9)
Zr–C(5)	2.456(7)	Zr–C(12)	2.484(7)	C(4)–C(5)	1.391(10)	C(11)–C(12)	1.377(9)
Zr–C(15)	2.164(8)	O–C(15)	1.153(8)	C(4)–C(7)	1.526(10)	C(11)–C(14)	1.503(10)

Bond Angles

C(1)–C(2)–C(3)	126.2(7)	C(3)–C(4)–C(7)	113.3(7)	C(9)–C(10)–C(11)	129.4(6)
C(1)–C(2)–C(6)	118.2(7)	C(5)–C(4)–C(7)	120.0(7)	C(10)–C(11)–C(12)	125.5(6)
C(3)–C(2)–C(6)	115.4(7)	C(8)–C(9)–C(10)	126.5(7)	C(10)–C(11)–C(14)	114.8(6)
C(2)–C(3)–C(4)	128.1(7)	C(8)–C(9)–C(13)	117.0(7)	C(12)–C(11)–C(14)	119.6(6)
C(3)–C(4)–C(5)	126.4(7)	C(10)–C(9)–C(13)	116.3(7)	Zr–C(15)–O	178.4(7)

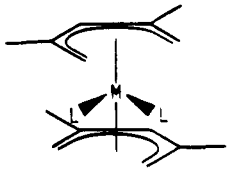

III

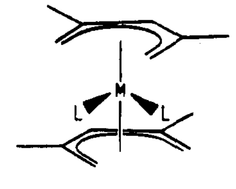

IV

are notably higher than those for $Zr(C_5H_5)_2(CO)_2$,[17] 1886 and 1975 cm^{-1}, and appear to indicate again that pentadienyl ligands are better accepting ligands than cyclopentadienyl. While this would not have been expected from the relative values of the ionization potentials and electron affinities, it is possible that the geometrically-required close positioning of the open dienyl plane to the metal leads to a significantly improved overlap for the δ-back-bonding interaction.

Structural Results and Discussion

Structural data for the syn-eclipsed $M(2,4\text{-}C_7H_{11})_2(L)$ complexes are provided in Tables II–VII and Figures 2–4. As has commonly been observed before, the structural studies generally reveal that dienyl C–C(X)–C bond angles become smaller for X = CH_3 relative to X = H and that the external dienyl C–C bonds are slightly shorter on average than the internal ones. These details do not seem to require further discussion for the present structures. The crystals of the $M(2,4\text{-}C_7H_{11})_2(PEt_3)$ (M = Zr, Nb) complexes are isomorphous and will be considered first. In each case (Figures 2 and 3), one finds the two dienyl planes to be slightly distorted from a parallel orientation (6.8 and 7.9°, respectively), with the PEt_3 ligands adopting their expected orientation, such that one arm is bent back, the other two to the sides. The fact that the one unique arm is situated between the terminal carbon atoms of one of the ligands leads to a positioning of the other two arms near the terminal carbon atoms (C(1), C(5)) of the other ligand. This appears to disturb the bonding in the first ligand (C(1)–C(5)) somewhat, as longer average[18] Zr–C (2.486(3) vs 2.433(3) Å) and Nb–C (2.418(3) vs 2.380 (3) Å) bonds are observed. From these data it would appear that the Zr(II) center is ca. 0.06 Å larger than Nb(II). On the other hand, the Zr–P and Nb–P bond lengths of 2.721(2) and 2.628(2) Å suggest a larger difference of ca. 0.09 Å. Data for the Mo(II) complex (vide infra) show further increases relative to Nb(II) by 0.07 and 0.11 Å. Most likely the M–P bonds are relatively weak and more influenced by the steric crowding in these molecules.

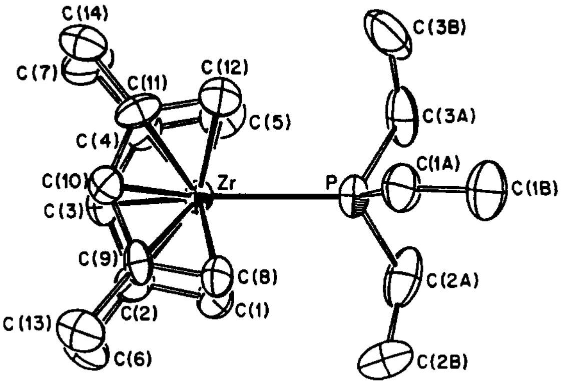

Figure 2. Solid-state structure of $Zr(2,4\text{-}C_7H_{11})_2(PEt_3)$.

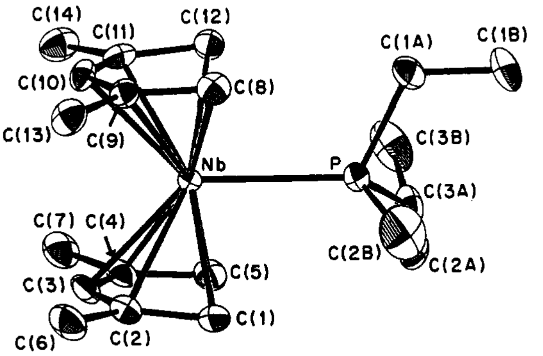

Figure 3. Solid-state structure of $Nb(2,4\text{-}C_7H_{11})_2(PEt_3)$.

The structure of $Zr(2,4\text{-}C_7H_{11})_2(CO)$ may be seen in Figure 4, and selected bonding parameters appear in Tables VI and VII. In this case there is a tilt of 1.9° between the two ligand planes, significantly less than those of the PEt_3 structures, for which the terminal CH_2 groups seemed to encounter significant repulsions from their phosphorus centers. As the result of the replacement of the PEt_3 ligand by CO, the molecular geometry is more symmetrical, essentially corresponding to that of C_{2v}. This leads to average Zr–C[1,5],[19] Zr–C[2,4], and Zr–C[3] bond lengths of 2.474(4), 2.447(3), and 2.424(4) Å, respectively.

Structural information for $Zr(2,4\text{-}C_7H_{11})_2(CO)_2$ may be found in Figure 5 and Tables VIII and IX. Actually, there are two crystallographically independent molecules, whose structural parameters are essentially identical. However, as suggested from the NMR spectra, the complex lacks any nontrivial symmetry elements, and one cannot really

---

(17) Demerseman, B.; Bouquet, G.; Bigorgne, M. *J. Organomet. Chem.* **1976**, *107*, C19.

(18) The esd's accompanying average values reflect the uncertainties of the average values, but not necessarily the distributions of the individual values.

(19) The use of brackets for carbon atom designations is meant to refer to average bonding parameters for the carbon atoms in those positions on the pentadienyl ligand(s).

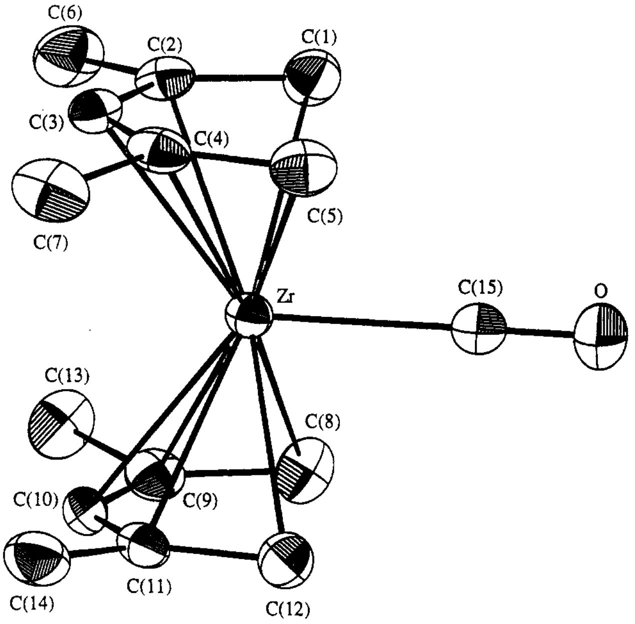

Figure 4. Solid-state structure of $Zr(2,4\text{-}C_7H_{11})_2(CO)$.

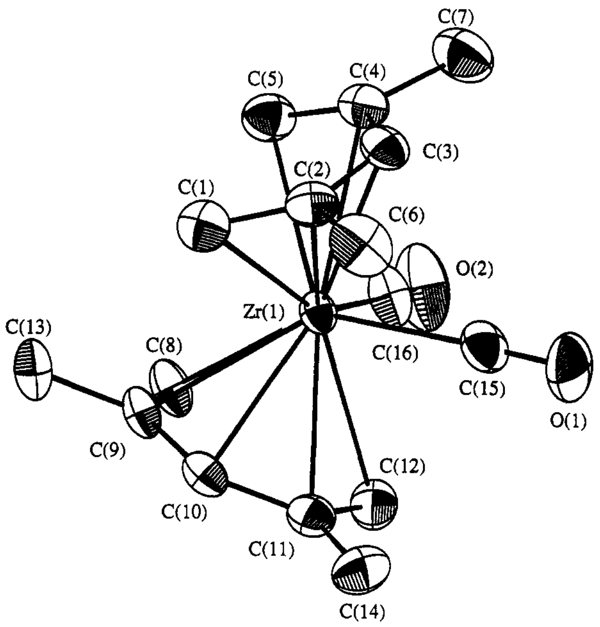

Figure 5. Solid-state structure of one of the two essentially identical but crystallographically independent $Zr(2,4\text{-}C_7H_{11})_2(CO)_2$ molecules.

Table VIII. Positional Parameters for the Non-Hydrogen Atoms of $Zr(2,4\text{-}C_7H_{11})_2(CO)_2$

atom	*x*	*y*	*z*
Zr(1)	0.19222(6)	0.73242(6)	0.10826(3)
Zr(1′)	−0.23061(6)	0.28681(6)	0.37899(3)
O(1)	0.5557(6)	0.8590(6)	0.0947(3)
O(1′)	−0.5493(6)	0.1570(7)	0.4618(3)
O(2′)	−0.4625(6)	0.5692(5)	0.3466(3)
O(2)	0.3343(7)	0.4283(6)	0.0193(3)
C(1)	−0.0119(8)	0.9457(7)	0.1227(3)
C(1′)	−0.0375(8)	0.0753(7)	0.3368(4)
C(2)	0.1251(8)	0.9952(6)	0.0905(3)
C(2′)	−0.1877(9)	0.0231(6)	0.3433(3)
C(3)	0.2013(8)	0.9294(7)	0.0298(3)
C(3′)	−0.3124(8)	0.0779(7)	0.3103(3)
C(4)	0.1589(8)	0.8049(7)	−0.0080(3)
C(4′)	−0.3163(8)	0.1964(7)	0.2684(3)
C(5)	0.0378(8)	0.7167(7)	0.0088(3)
C(5′)	−0.1966(8)	0.2896(7)	0.2543(3)
C(6)	0.206(1)	1.1196(7)	0.1209(4)
C(6′)	−0.225(1)	−0.0966(8)	0.3893(4)
C(7)	0.273(1)	0.7585(9)	−0.0693(4)
C(7′)	−0.4701(8)	0.2285(9)	0.2428(3)
C(8)	0.0317(8)	0.5275(7)	0.1558(3)
C(8′)	−0.0580(8)	0.5054(7)	0.3786(3)
C(9)	−0.0020(7)	0.6536(6)	0.1971(3)
C(9′)	0.0238(7)	0.3920(7)	0.4023(3)
C(10)	0.1090(7)	0.7353(6)	0.2287(3)
C(10′)	−0.0301(7)	0.3085(7)	0.4573(3)
C(11)	0.2738(7)	0.7176(7)	0.2221(3)
C(11′)	−0.1762(7)	0.3213(7)	0.4963(3)
C(12)	0.3589(8)	0.6046(8)	0.1818(3)
C(12′)	−0.2968(8)	0.4248(7)	0.4872(3)
C(13)	−0.1722(8)	0.7069(8)	0.2094(4)
C(13′)	0.1842(8)	0.342(1)	0.3654(4)
C(14)	0.3623(8)	0.8299(8)	0.2578(3)
C(14′)	−0.2055(9)	0.2134(9)	0.5494(3)
C(15)	0.4315(8)	0.8161(7)	0.0984(3)
C(15′)	−0.4404(8)	0.1988(8)	0.4329(3)
C(16)	0.2904(8)	0.5319(7)	0.0488(3)
C(16′)	−0.3865(7)	0.4729(7)	0.3576(3)

average many of the bonding parameters (e.g., compare Zr–C(1) with Zr–C(5) and Zr–C(8) with Zr–C(12)). It can be seen, however, that the Zr–C bond lengths for the second ligand(s) are ca. 0.03 Å shorter than those for the first and that these lengths are significantly longer on the average (ca. 0.06 Å) than those for the monocarbonyl. As noted earlier, in related $M(allyl)_2L_2$, $M(diene)_2L_2$, and $Zr(C_6H_7)_2(dmpe)$ complexes, the additional ligands L generally reside by the open edges of the organic groups, which would lead to C_2 symmetry. In this case, however, the presence of the methyl groups seems to destabilize such an orientation, with the result that one carbonyl resides by an open edge, the other by the backside of a dienyl ligand. Not surprisingly, it is this latter ligand, with its unusual orientation, which has the longer Zr–C bonds. However, the corresponding carbonyl (C(15), C(15′)) seems to bond more strongly than the "correctly" positioned one (C(16), C(16′)), the respective average Zr–C bond lengths being 2.208(4) vs 2.236(3) Å. This occurs despite the fact that C(15) and C(15′) encounter more steric repulsion with the methyl groups than do C(16) and C(16′). Hence, the backside orientation may aid the carbonyl bonding, while diminishing the dienyl bonding. It is also interesting to compare these data with the data for $Zr(C_5H_5)_2(CO)_2$[20] and $Zr(C_5Me_5)_2(CO)_2$.[21] The structures are actually remarkably similar, having tilts between the organic ligands of 140.7, 141, and 147.4° and OC–Zr–CO angles of 88.1, 89.2, and 86.1°, respectively. The average dienyl M–C bond lengths are actually also quite similar at 2.48–2.50 Å. However, the Zr–CO bond lengths in the open complex are significantly longer than those in $Zr(C_5H_5)_2(CO)_2$ (2.16 Å) and $Zr(C_5Me_5)_2(CO)_2$ (2.145 Å), which could be attributed either to the greater steric demands of the open ligand[22] or to the greater accepting properties of pentadienyl relative to cyclopentadienyl ligands.[23]

The structure and structural parameters for $Mo(2,4\text{-}C_7H_{11})_2(PEt_3)$ are provided in Figure 6 and Tables X and XI. Certainly the most noticeable feature here is the presence of one η^5-S-2,4-C_7H_{11} (S = sickle) ligand, which results in the lack of any nontrivial symmetry elements.

---

[20] Atwood, J. L.; Rogers, R. D.; Hunter, W. E.; Floriani, C.; Fachinetti, G.; Chiesi-Villa, A. *Inorg. Chem.* **1980**, *19*, 3812.

[21] Sikora, D. J.; Rausch, M. D.; Rogers, R. D.; Atwood, J. L. *J. Am. Chem. soc.* **1981**, *103*, 1265.

[22] Freeman, J. W.; Hallinan, N. C.; Arif, A. M.; Gedridge, R. W.; Ernst, R. D.; Basolo, F. *J. Am. Chem. Soc.* **1991**, *113*, 6509.

[23] (a) Liu, J.-Z.; Ernst, R. D. *J. Am. Chem. Soc.* **1982**, *104*, 3737. (b) Ernst, R. D.; Liu, J.-Z.; Wilson, D. R. *J. Organomet. Chem.* **1983**, *250*, 257.

Table IX. Pertinent Bond Distances (Å) and Angles (deg) for $Zr(2,4\text{-}C_7H_{11})_2(CO)_2$

Bond Distances			
Zr(1)–C(1)	2.569(4)	C(1)–C(2)	1.387(6)
Zr(1)–C(2)	2.531(4)	C(2)–C(3)	1.430(6)
Zr(1)–C(3)	2.493(4)	C(2)–C(6)	1.500(7)
Zr(1)–C(4)	2.545(4)	C(3)–C(4)	1.427(6)
Zr(1)–C(5)	2.539(4)	C(4)–C(5)	1.367(6)
Zr(1)–C(8)	2.555(4)	C(4)–C(7)	1.535(7)
Zr(1)–C(9)	2.486(4)	C(8)–C(9)	1.401(5)
Zr(1)–C(10)	2.485(4)	C(9)–C(10)	1.419(5)
Zr(1)–C(11)	2.506(4)	C(9)–C(13)	1.510(5)
Zr(1)–C(12)	2.495(4)	C(10)–C(11)	1.404(6)
Zr(1)–C(15)	2.207(5)	C(11)–C(12)	1.420(6)
Zr(1)–C(16)	2.242(5)	C(11)–C(14)	1.506(6)
O(1)–C(15)	1.143(5)	O(2)–C(16)	1.131(5)
Zr(1′)–C(1′)	2.562(4)	C(1′)–C(2′)	1.384(6)
Zr(1′)–C(2′)	2.506(4)	C(2′)–C(3′)	1.415(6)
Zr(1′)–C(3′)	2.485(4)	C(2′)–C(6′)	1.513(6)
Zr(1′)–C(4′)	2.551(4)	C(3′)–C(4′)	1.430(6)
Zr(1′)–C(5′)	2.533(4)	C(4′)–C(5′)	1.379(6)
Zr(1′)–C(8′)	2.544(4)	C(4′)–C(7′)	1.493(6)
Zr(1′)–C(9′)	2.494(4)	C(8′)–C(9′)	1.378(6)
Zr(1′)–C(10′)	2.471(4)	C(9′)–C(10′)	1.444(6)
Zr(1′)–C(11′)	2.493(4)	C(9′)–C(13′)	1.535(6)
Zr(1′)–C(12′)	2.486(4)	C(10′)–C(11′)	1.405(5)
Zr(1′)–C(15′)	2.208(5)	C(11′)–C(12′)	1.416(6)
Zr(1′)–C(16′)	2.231(4)	C(11′)–C(14′)	1.523(6)
O(1′)–C(15′)	1.141(5)	O(2′)–C(16′)	1.130(5)

Bond Angles			
C(15)–Zr(1)–C(16)	88.1(2)	C(15′)–Zr(1′)–C(16′)	87.2(2)
Zr(1)–C(15)–O(1)	178.4(4)	Zr(1′)–C(15′)–O(1′)	178.0(4)
Zr(1)–C(16)–O(2)	177.2(4)	Zr(1′)–C(16′)–O(2′)	178.4(4)
C(1)–C(2)–C(3)	123.6(4)	C(1′)–C(2′)–C(3′)	123.6(3)
C(1)–C(2)–C(6)	120.1(3)	C(1′)–C(2′)–C(6′)	119.3(3)
C(3)–C(2)–C(6)	116.3(3)	C(3′)–C(2′)–C(6′)	117.1(3)
C(2)–C(3)–C(4)	129.0(3)	C(2′)–C(3′)–C(4′)	129.7(4)
C(3)–C(4)–C(5)	126.5(4)	C(3′)–C(4′)–C(5′)	126.2(4)
C(3)–C(4)–C(7)	115.2(4)	C(3′)–C(4′)–C(7′)	116.0(4)
C(5)–C(4)–C(7)	117.9(4)	C(5′)–C(4′)–C(7′)	117.6(4)
C(8)–C(9)–C(10)	125.9(4)	C(8′)–C(9′)–C(10′)	126.3(4)
C(8)–C(9)–C(13)	117.0(4)	C(8′)–C(9′)–C(13′)	118.1(4)
C(10)–C(9)–C(13)	117.0(4)	C(10′)–C(9′)–C(13′)	115.6(4)
C(9)–C(10)–C(11)	129.0(4)	C(9′)–C(10′)–C(11′)	128.0(4)
C(10)–C(11)–C(12)	123.5(4)	C(10′)–C(11′)–C(12′)	123.6(4)
C(10)–C(11)–C(14)	116.9(4)	C(10′)–C(11′)–C(14′)	117.1(4)
C(12)–C(11)–C(14)	119.5(4)	C(12′)–C(11′)–C(14′)	119.3(4)

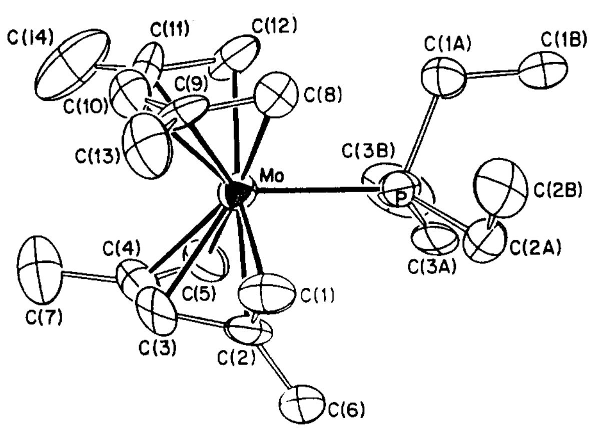

Figure 6. Solid-state structure of $Mo(2,4\text{-}C_7H_{11})_2(PEt_3)$.

Table X. Positional Parameters for the Non-Hydrogen Atoms of $Mo(2,4\text{-}C_7H_{12})_2(PEt_3)$

atom	*x*	*y*	*z*
Mo	0.5505(1)	0.3937(1)	0.8581(0)
P	0.7103(3)	0.3590(3)	0.9261(2)
C(1)	0.5230(16)	0.2397(12)	0.8441(7)
C(2)	0.6070(14)	0.2766(9)	0.8109(6)
C(3)	0.5527(13)	0.3449(13)	0.7743(6)
C(4)	0.6041(14)	0.4264(13)	0.7678(6)
C(5)	0.6987(14)	0.4508(11)	0.8000(5)
C(6)	0.7281(16)	0.2324(11)	0.7995(6)
C(7)	0.5526(14)	0.4940(14)	0.7256(7)
C(8)	0.4219(13)	0.3714(11)	0.9264(6)
C(9)	0.3515(14)	0.3908(10)	0.8784(7)
C(10)	0.3707(13)	0.4710(12)	0.8545(7)
C(11)	0.4600(14)	0.5414(12)	0.8596(7)
C(12)	0.5464(15)	0.5341(11)	0.9007(7)
C(13)	0.2550(16)	0.3225(15)	0.8609(7)
C(14)	0.4629(17)	0.6180(13)	0.8202(13)
C(1A)	0.6975(13)	0.4255(10)	0.9884(6)
C(1B)	0.7892(17)	0.4069(10)	1.0323(7)
C(2A)	0.7288(15)	0.2391(11)	0.9530(6)
C(2B)	0.6253(18)	0.2087(12)	0.9911(7)
C(3A)	0.8670(17)	0.3804(10)	0.9092(6)
C(3B)	0.8985(16)	0.4854(13)	0.9025(8)

While this complex is the first case in which η^5-S-pentadienyl coordination is clearly favored relative to the more normal η^5-U form, some η^5-S complexes could be generated at temperatures low enough to prevent isomerization, and in the case of $Fe(1,1,5\text{-}(CH_3)_3C_5H_4)(CO)_3^+$, the presence of the three methyl substituents on the terminal carbon atoms of the open ligand leads to sufficient destabilization of the η^5-U form that an equilibrium between the η^5-S and the η^5-U forms results.[24] Subsequently, additional examples of such coordination to molybdenum have been found,[25] as well as to other metals, as in $Cr(C_5H_5)$(pentadienyl)(L),[22,26] $W(2,4\text{-}C_7H_{11})_2(PEt_3)$,[27] $W(\text{dienyl})(CO)_3Br$,[28] and $Re(C_5Me_5)(\text{dienyl})Cl$[29] complexes. The extent of the distortion may best be gauged by the value of the C(4)–C(3)–C(2)–C(1) and C(4)–C(3)–C(2)–C(6) torsion angles, 47.6 and 65.1°, respectively. Such twisting would be expected to decrease the conjugation between the two ends of the ligand, and indeed one can observe a particularly long C(2)–C(3) bond, 1.481(22) Å, consistent with the participation of an allyl–ene coordination mode, V. This suggests a connection with some bis(olefin) complexes, such as $Ru(C_5Me_5)(3\text{-}R_3SiO\text{-}1,4\text{-}C_5H_7)$ (C_5H_7 = pentadiene),[30] in which the two olefins are oriented in a mixed "‖–⊥" mode (VI) rather than an all-parallel mode (VII). It can be seen that $Mo(2,4\text{-}C_7H_{11})_2(PEt_3)$ is related to VI, in that the allyl and ene

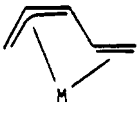

V

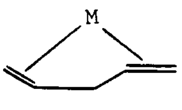

VI

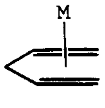

VII

---

(24) (a) Mahler, J. E.; Pettit, R. *J. Am. Chem. Soc.* **1963**, *85*, 3955. (b) Clinton, N. A.; Lillya, C. P. *Ibid.* **1970**, *92*, 3065. (c) Sorensen, T. S.; Jablonski, C. R. *J. Organomet. Chem.* **1970**, *25*, C62. (d) Brookhart, M.; Harris, D. L. *Ibid.* **1972**, *42*, 441.

(25) (a) Lee, G. H.; Peng, S.-M.; Lee, T.-W.; Liu, R.-S. *Organometallics* **1986**, *5*, 2378. (b) Green, M.; Nagle, K. R.; Woolhouse, C. M.; Williams, D. J. *J. Chem. Soc., Chem. Commun.* **1987**, 1793.

(26) Waymouth, R. M. Private communication.

(27) Stahl, L.; Ziegler, M. L.; Ernst, R. D. Unpublished results.

(28) Sivavec, T. M.; Katz, T. J.; Chiang, M. Y.; Yang, X.-Q. *Organometallics* **1989**, *8*, 1620.

(29) Herrmann, W. A.; Fischer, R. A.; Herdtweck, E. *Organometallics* **1989**, *8*, 2821.

(30) Trakarnpruk, W.; Rheingold, A.; Ernst, R. D. Unpublished results.

Table XI. Selected Bond Distances (Å) and Angles (deg) for Mo(2,4-C_7H_{11})$_2$(PEt_3)

Bond Distances

Mo–C(1)	2.283(17)	Mo–C(8)	2.260(15)	C(1)–C(2)	1.366(23)	C(8)–C(9)	1.465(23)
Mo–C(2)	2.163(14)	Mo–C(9)	2.295(16)	C(2)–C(3)	1.481(22)	C(9)–C(10)	1.326(23)
Mo–C(3)	2.208(16)	Mo–C(10)	2.314(15)	C(3)–C(4)	1.327(26)	C(10)–C(11)	1.437(23)
Mo–C(4)	2.382(16)	Mo–C(11)	2.374(17)	C(4)–C(5)	1.380(22)	C(11)–C(12)	1.417(24)
Mo–C(5)	2.359(15)	Mo–C(12)	2.300(17)	C(2)–C(6)	1.532(23)	C(9)–C(13)	1.533(24)
P–C(1A)	1.837(15)	Mo–P	2.523(4)	C(4)–C(7)	1.551(25)	C(11)–C(14)	1.486(30)
P–C(2A)	1.878(17)	C(1A)–C(1B)	1.529(23)	C(2A)–C(2B)	1.565(25)	C(3A)–C(3B)	1.573(24)
P–C(3A)	1.838(19)						

Bond Angles

C(1)–C(2)–C(3)	110.6(14)	C(3)–C(4)–C(7)	119.0(15)	C(10)–C(9)–C(13)	123.8(15)
C(1)–C(2)–C(6)	124.3(13)	C(5)–C(4)–C(7)	121.4(16)	C(10)–C(11)–C(12)	119.4(15)
C(2)–C(3)–C(4)	119.6(14)	C(8)–C(9)–C(10)	116.6(14)	C(10)–C(11)–C(14)	119.2(16)
C(3)–C(2)–C(6)	122.1(13)	C(8)–C(9)–C(13)	119.4(14)	C(12)–C(11)–C(14)	121.3(16)
C(3)–C(4)–C(5)	119.5(15)	C(9)–C(10)–C(11)	134.3(15)	Mo–P–C(1A)	114.2(5)
P–C(1A)–C(1B)	117.5(11)	P–C(3A)–C(3B)	113.8(12)	Mo–P–C(2A)	120.3(5)
P–C(2A)–C(2B)	113.4(11)			Mo–P–C(3A)	119.6(5)

fragments adopt the ∥–⊥ orientation, rather than an all-parallel one, which would entail the more normal η^5-U coordination. In accord with earlier arguments, it appears that the occurrence of the η^5-S bonding mode is due to electronic rather than steric factors.[22,31]

The sickle conformation leads to rather irregular patterns in the bonding. The Mo–C(2,3) bonds are shortest, with the outer Mo–C bonds becoming longer, a situation reminiscent of Cr(C_5H_5)(C_5H_7)(CN-2,6-(CH_3)$_2$$C_6H_3$).[22] This presumably reflects the difficulties in bringing about effective bonding simultaneously to the two ends. Another indication of this may be found in the relatively small values of the C(1)–C(2)–C(3), C(2)–C(3)–C(4), and C(3)–C(4)–C(5) bond angles, which range from 110.6(14)–119.6(14)°. These small angles seem to prevent the ends from being separated even further.

Conclusion

With the incorporation of 1 or 2 equiv of a Lewis base, stable 16-, 17-, and 18-electron open metallocene complexes may be isolated for the second- and third-row transition metals zirconium, hafnium, niobium, and molybdenum. The fact that even the electron-deficient zirconium and hafnium mono(ligand) complexes are generally reluctant to add a second Lewis base provides a further clear indication of the greatly enhanced steric demands of pentadienyl ligands relative to C_5H_5 and even C_5Me_5. While it is not entirely clear what leads to the stabilization of η^5-S pentadienyl coordination for molybdenum, it is at least evident that electronic factors are involved. Finally, whether or not 17-electron Ta(2,4-C_7H_{11})$_2$(L) complexes may also be obtained remains to be determined.

Acknowledgment. R.D.E. expresses his gratitude for support of this research from the National Science Foundation.

Supplementary Material Available: Tables of atom deviations from least-squares planes and hydrogen atom and anisotropic thermal parameters for the diffraction studies (17 pages). Ordering information may be found on any current masthead page.

OM920673T

---

(31) Shen, J. K.; Freeman, J. W.; Hallinan, N. C.; Rheingold, A. L.; Arif, A. M.; Ernst, R. D.; Basolo, F. *Organometallics* **1992**, *11*, 3215.